very broad range of excitation energies. The slope of the line corresponds to about 25 MeV/charge. Since the total mass loss is about twice the evaporated charge (within experimental erors), one obtains an average energy loss per particle of ~12.5 MeV, which is consistent with simple estimates assuming evaporation. Of course, we have only considered symmetric products at angles behind the grazing angle. The situation may be more complicated for Z's below the projectile, where there are indications that high-energy particles are emitted.[16]

In conclusion, the technique of simultaneous Z identification of the major fragments is a powerful tool for studying deep-inelastic processes since it directly provides the multiplicity of the evaporated charge. The data support the view that the dissipated kinetic energy is thermalized in both fragments and that they dispose of their excitation energy by evaporating light particles. This picture seems to be valid over a broad range of bombarding energies as evidenced by the fact that the energy loss per nucleon does not vary strongly as it might if nonequilibrium particle emission became a dominant mechanism at high energies. Thus it appears that most of the available phase space for the intrinsic degrees of freedom of the fragments appears to be explored in deep-inelastic processes.

This work was supported by the Division of Nuclear Physics of the U. S. Department of Energy.

[a]Present address: Laboratoire de Physique Corpusculaire, Université de Caen, 14000 Caen, France.

[1]W. U. Schröder and J. R. Huizenga, Annu. Rev. Nucl. Sci. 27, 465 (1977).

[2]L. G. Moretto and R. Schmitt, J. Phys. (Paris) 37, 109 (1976).

[3]R. A. Broglia, C. H. Dasso, and A. Winter, Phys. Lett. 61B, 113 (1976).

[4]K. Albrecht and W. Stocker, Nucl. Phys. A278, 95 (1977).

[5]J. Randrup, Lawrence Berkeley Laboratory Report No. LBL-5847, 1976 (to be published).

[6]M. Ho *et al.*, Z. Phys. A283, 235 (1977).

[7]A. Gamp *et al.*, Phys. Lett. 74B, 215 (1978).

[8]J. W. Harris *et al.*, Phys. Rev. Lett. 38, 1460 (1977).

[9]J. M. Miller *et al.*, Phys. Rev. Lett. 40, 100 (1978).

[10]C. K. Gelbke *et al.*, Phys. Lett. 71B, 83 (1977).

[11]B. Cauvin *et al.*, to be published.

[12]R. Babinet *et al.*, Nucl. Phys. A296, 160 (1978).

[13]C. K. Gelbke *et al.*, Nucl. Phys. A269, 460 (1976).

[14]G. J. Mathews *et al.*, Lawrence Berkeley Laboratory Report No. LBL-5075, 1976 (unpublished).

[15]L. G. Moretto, in Proceedings of the IPCR Symposium on Macroscopic Features of Heavy-Ion Collisions and Pre-equilibrium Processes, Hakone, Japan, 1977, edited by H. Kamitsubo and M. Ishihara (to be published).

[16]R. P. Schmitt *et al.*, Lawrence Berkeley Laboratory Report No. LBL-7754, 1978 (unpublished).

^{3}He and ^{4}He Form Factors and the Dimensional-Scaling Quark Model

Benson T. Chertok
American University, Washington, D. C. 20016
(Received 2 March 1978)

The large-q^2 behavior of new elastic electron-scattering measurements from ^{3}He and ^{4}He is compared with the dimensional-scaling quark model. The slope change in $F_{^3\mathrm{He}}/F_{\mathrm{quark}}$ for $q^2 > 2$ GeV^2 when compared to ^{2}H and ^{4}He is conjectured to be evidence for scaling permitting the further synthesis of nucleon-nucleon and quark-gluon physical ideas.

With the appearance of large-momentum-transfer data on the nuclei ^{2}H, ^{3}He, and ^{4}He from elastic electron scattering together with measurements of nucleon-nucleon and nucleon-deuteron elastic scattering at 90° in the same range, $q^2 > 1$ GeV^2, it should be possible to make significant progress in understanding the nuclear force and the substructure of nuclei for $r \sim 1/q \sim 0.2$ fm.[1] The purpose of this Letter is to examine the new large-q^2 data[2] of the elastic form factors of ^{3}He and ^{4}He in terms of the dimensional-scaling quark model (DSQM). An impressive body of nuclear particle reactions is described by the theory when $s, t, u \gg M^2$.[3] The new helium data are not yet in the asymptotic region but they should be interpretable in terms of our simple refinements to the DSQM.[4,5]

The principal ideas of this model are *dimensional scaling* of high-energy amplitudes using quark counting, leading to the prediction for the

nucleon and light nuclei that $F_A \sim (q^2)^{1-3A}$ for $q^2 \gg M^2$, and the dominance of the *constituent-interchange* force between quarks of different nucleons to share q/A so that, for example, the reduced or structureless deuteron form factor $f_d = F_d / F_p^2(q^2/4) \simeq (1+q^2/\frac{6}{5}\beta^2)^{-1} \sim (q^2)^{-1}$.[5] The contention is that the quark-interchange model (QIM) diagram contains the important dynamics for elastic nuclear form factors at large q^2. Thus it is similar to if not the same as particular meson-exchange-current (MEC) diagrams which are being explored currently in nuclear calculations.

It has been reported that the shape of $F_{^3\mathrm{He}}$ and $F_{^4\mathrm{He}}$ predicted from the refined DSQM was not observed experimentally for $1 < q^2 < 2.2$ GeV^2 although the sparse data beyond $q^2 \gtrsim 2$ GeV^2 (2.25–3 GeV^2) in ^{3}He could be exhibiting this shape.[2] From the present analysis, the following results are deduced. On the basis of a change in slope of $F_{^3\mathrm{He}}/F_{\mathrm{quark}}$ for $q^2 > 2$ GeV^2, it is hypothesized that scaling due to the underlying nine-quark structure has been observed. The ramifications of this are developed. They are (1) the determination of the mass scale, q_0^2, for the threshold of dimensional scaling of nuclear elastic electromagnetic form factors; (2) the significant improvement in the comparison of nuclear theory with experiment as in Fig. 3; and (3) the first evaluation utilizing large-q^2 reactions of the wave function densities at the origin, $\psi_{^2\mathrm{H}}^2(0)/\psi_{^3\mathrm{He}}^2(0,0)$.

The refinements to the DSQM have been described.[4] For the explicit nucleon-dinucleon structure in Fig. 1(a), we have $F_{^3\mathrm{He}} \sim F_p(q^2/9) \times F_d(4q^2/9)[1+q^2/\frac{9}{8}\beta^2]^{-1}$. The approximate sign allows for the normalization as well as nonleading terms which have been omitted. $\psi^2(0,0)$ for the three-nucleon structure will be evaluated phenomenologically in Eq. (6). An alternative chain model for $3A-1$ transfers of momentum has been developed with an underlying mass scale $M_0^2(n) = n\beta^2$ where the constant $\beta^2 = 0.235$ GeV^2 has been set by the measured pion form factor. An example of this diagram is given in Fig. 1(b). Calculation of the leading term for the underlying three-nucleon structure yields the prediction (hereafter F_{QIM}),

$$F_{^3\mathrm{He}} \sim F_p^3\left(\frac{q^2}{9}\right)\left[1+\frac{q^2}{\frac{9}{8}\beta^2}\right]^{-1}\left[1+\frac{q^2}{\frac{27}{10}\beta^2}\right]^{-1} \qquad (1)$$

with two quark interchanges of $q/3$.[6] Partitioning q in the chain model, Fig. 1(b), yields the prediction which can be approximated as

$$F_{^3\mathrm{He}} \sim (1+q^2/9\beta^2)^{-8}. \qquad (2)$$

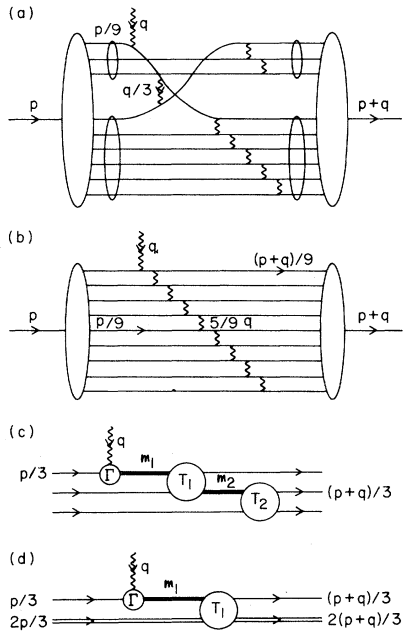

FIG. 1. Different views of the ^{3}He form factor at large q^2: (a) constituent-interchange model with explicit nucleon-dinucleon substructure; (b) democratic chain model; (c) off-shell nucleon-nucleon-nucleon scattering; (d) off-shell nucleon-nucleus scattering.

As required, these three predictions are asymptotically consistent with dimensional counting, $F_{^3\mathrm{He}} \sim (q^2)^{-8}$. Similarly $F_{^4\mathrm{He}}$ can be described as a skeletal four-nucleon structure, n-^{3}He, d-d, or chain of twelve quarks.

The expressions for the nuclear form factor in Eq. (1) and nucleon-dinucleon above should be related to meson-exchange currents in nuclear physics calculations. However, the origins of these approaches are entirely different; for example, here one employs Bjorken scaling, dimensional counting, quark identification for the quantum fields, and finiteness of the bound-state wave function at the origin.

The three predictions for ^{3}He are compared with the data which has been observed to fall off approximately exponentially, $F_{^3\mathrm{He}} = 0.03e^{-2.7q^2}$, with a reduced χ^2 of 1.03 for $0.8 \leq q^2 \leq 3.0$ GeV^2.[2,7] Evidence for the validity of the model is the q^2 independence of the ratio of experiment to theory. Although scaling can be clearly ruled out for $1 < q^2 < 2$ GeV^2, beyond 2 GeV^2 there is a flattening out in ^{3}He as in Fig. 2. This effect is observed for the three predictions. We conjecture that this

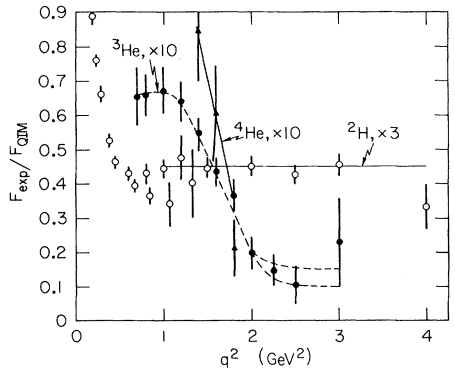

FIG. 2. Form-factor data for ^{2}H, ^{3}He, and ^{4}He compared to quark- or constituent-interchange model predictions in Ref. 4 [Eqs. (37)–(39)] and Eq. (1).

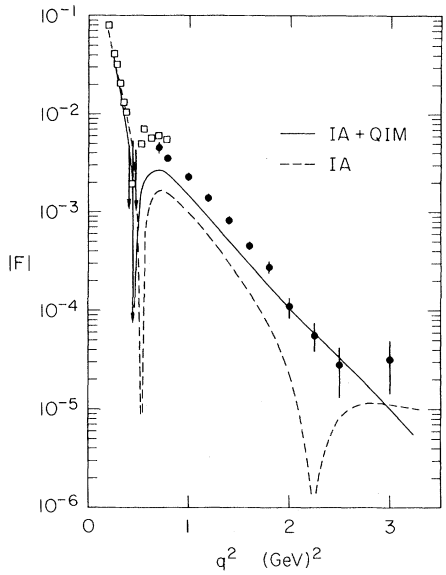

FIG. 3. ^{3}He form factor compared to nonrelativistic impulse approximation (IA) and IA augmented by the quark-interchange model.

change in slope is evidence for the onset of scaling in ^{3}He for $q^2 > 2$ GeV^2 and shall explore the consequences.

In Fig. 2 the elastic form-factor data are displayed for the three basic atomic nuclei—^{2}H, ^{3}He, and ^{4}He, compared to the extended DSQM prediction, e.g., Eq. (1) for ^{3}He. The observations are a change in slope followed by scaling for ^{2}H beyond $q^2 \sim 1$ GeV^2 with an "asymptote" of 0.15, the change in slope and conjectured scaling for ^{3}He with a normalization of 0.010 to 0.015, and the rapid falloff for ^{4}He, which is the nearly vertical solid line, out to the boundary at 1.8 GeV^2. This leads to the first new result, namely that the *onset of scaling* given by the democratic chain model, $F_n \sim (1 + q^2/n\beta^2)^{1-n}$ with $n\beta^2 = 0.7$, 1.4, 2.1, and 2.8 GeV^2 for $A = n/3$ of 1, 2, 3, and 4, respectively, is a reasonable working guide. That is, the q^2 threshold for scaling is

$$q_0^2 \sim 0.71A \text{ GeV}^2. \tag{3}$$

Next the scaling hypothesis for $F_{^3\text{He}}$ can be utilized in the comparison between nuclear theory and experiment at much lower q^2. A nonrelativistic impulse-approximation calculation, the Reid soft-core potential used as input to the Faddeev equation,[8] is displayed by the dashed curve in Fig. 3. The well-known discrepancies at $q^2 < 1$ GeV^2 are the diffraction minimum at 0.53 GeV^2 instead of the experimental observation at 0.45 GeV^2 shown by the vertical arrows, and the factor of 3 underestimate in the height of the secondary maximum. I augment F_{IA} by the QIM result of Eq. (1) (with the normalization from Fig. 2), that is,

$$F_{^3\text{He}} = F_{IA} + F_{QIM}. \tag{4}$$

The further assumption that the QIM amplitude is negative will require future theoretical confirmation. This will be possible when fully covariant calculations which include the quark-interchange diagram are carried out. Meanwhile one can argue that this choice of sign relative to the impulse-approximation amplitude should be the same for the charge form factors of ^{2}H, ^{3}He, and ^{4}He. Indeed this choice is in the right direction to improve the agreement with experiment in each case. The results displayed in Fig. 3 by the solid line indicate improved agreement with experiment everywhere beyond 0.35 GeV^2 including a shift of the minimum down to 0.46 GeV^2 and secondary-maximum increase of 180%. With the obvious caveats that relativistic and other refinements to F_{IA} could be large, nevertheless it is clear that F_{QIM} for ^{3}He of the magnitude and q^2 shape deduced here could be supplying the missing ingredient to nuclear theory.

Next the calculation of the normalization of $F_{^3\text{He}}$ in the context of the refined dimensional scaling is described. If the ^{3}He form factor is asymptotic in the limited sense of Fig. 2, then the relativistic bound-state wave function $\psi_{^3\text{He}}(x,y)$ can be estimated at x_μ and $y_\mu = 0$.[9] One calculates the amplitudes for

$$\gamma_v + p + (n+p) \to p' + (n'+p') \tag{5}$$

and, for example, $\gamma_v + p + d \to p' + d'$ using elastic-scattering data for $np \to np$, $pp \to pp$, and $pd \to pd$

for $s,t,u \gg M^2$. Using the diagram in Fig. 1(c) gives

$$F_{^3\mathrm{He}} \sim \frac{6\Gamma\Delta(\mathfrak{M}_1^2)T_1\Delta(\mathfrak{M}_2^2)T_2\psi_{^3\mathrm{He}}{}^2}{F_N(q'^2)}(0,0), \qquad (6)$$

where the T-matrix amplitudes for NN scattering at large t and $\theta = 90°$ can be reduced (see Eq. 28 of Ref. 5) and

$$T_{NN}(t)/F_N{}^2(t/4) \simeq 320 \pm 60 \qquad (7)$$

by averaging over the np and pp elastic-scattering cross sections. The extrapolation off shell is made as previously for $T_1(q^2) = T(t = \frac{4}{9}q^2, \mathfrak{M}_1{}^2)$ and $T_2(q^2) = T(t = q^2/9, \mathfrak{M}_2{}^2)$, where $\mathfrak{M}_1{}^2 = \frac{2}{3}q^2$ and $\mathfrak{M}_2{}^2 = \frac{2}{9}q^2$. Double counting of the middle nucleon in Fig. 1(c) is removed by $F_N{}^{-1}$, the nucleon form factor in Eq. (6), evaluated at $q'^2 = q^2/9$. In Eq. (6), there are six time-ordered diagrams like Fig. 1(c), $\Gamma(q^2)\Delta(\mathfrak{M}_1{}^2) \sim \mathfrak{M}_1{}^{-2}$, $\Delta(\mathfrak{M}_2{}^2) \sim \mathfrak{M}_2{}^{-2}$, and $(q^2)^8 F_{^3\mathrm{He}}$ can be estimated using the large-q^2 limit from Eq. (1) with Fig. 2. Dimensional counting of the right-hand side of Eq. (6) gives $(q^2)^{-8}$ as required.

In the absence of large-t pd elastic-scattering data at $\theta \sim 90°$, the amplitude in Fig. 1(d) can be evaluated using Eq. (7) in its off-shell form, together with F_d, the deuteron form factor.[10] This contribution to $F_{^3\mathrm{He}}$ is much smaller than from Eq. (6). The result from substituting the off-shell values of T and the estimated asymptote of $F_{^3\mathrm{He}}$ into Eq. (6) is

$$\psi_{^3\mathrm{He}}{}^2(0,0) \sim 3 \times 10^{-10}\ \mathrm{GeV}^4 \qquad (8)$$

within characteristic sizes $\Delta x, \Delta y \sim 1/q_{\max} = 0.1$ fm. The equivalent nonrelativistic result, using $\psi_{\mathrm{NR}}{}^2(0,0) \sim (2M)^2\psi^2(0,0)$, is approximately 1×10^{-9} GeV^6. The ratios of ψ^2 for the deuteron and ^{3}He are more certain; the relativistic result is

$$\psi_d{}^2(0)/\psi_{^3\mathrm{He}}{}^2(0,0) \approx 10^4\ \mathrm{GeV}^{-2}, \qquad (9)$$

and the same ratio in the nonrelativistic limit (NR) is

$$\left.\frac{\psi_d{}^2(0)}{\psi_{^3\mathrm{He}}{}^2(0,0)}\right|_{\mathrm{NR}} \approx 5300\ \mathrm{GeV}^{-3} = 41\ \mathrm{fm}^3. \qquad (10)$$

It has been noted that $\psi_d(0)|_{\mathrm{NR}}$ is comparable in order of magnitude to the wave function of soft-core potentials.[5]

The ratio in Eq. (10) can be examined in the hierarchy of composite systems, i.e., six- vs nine-quark states, single-nucleon distribution in proceeding from ^{2}H to ^{3}He, and at the nuclear level of $A = 2$ compared to $A = 3$. Calculations of structured graphs of these $3A$-quark states will require explicit use of the quark flavor, spin, and color degrees of freedom.[11] A comparison of Eq. (10) with contemporary wave functions generated from one-boson-exchange potentials for ^{2}H and ^{3}He would be interesting. A plausible yet very simple comparison with Eq. (10) at the nucleon level would be a constant-density model for internucleon distances to r, $\rho \sim 2/q_{\max} \sim 0.2$ to 0.3 fm. In this severely overlapped or interpenetrating configuration of nucleons, the resulting ratio of probabilities is determined to be

$$P(0)/P(0,0) \sim 10^3. \qquad (11)$$

The large repulsion in adding a single nucleon to the overlapped N-N system presumably reflects the strong underlying N-N repulsion at short distance. At the quark-constituent level this repulsion could be attributable to the increased number of fermion degrees of freedom. The consideration of the result of Eq. (10) at the nucleus level is to inquire whether possibly the charge or matter distributions reflect this ratio. The rms radius for a N-N pair extracted from such a comparison yields $a_{\mathrm{ch}} \sim 2.4$ fm and $a_m \sim 2.2$ fm, which is not greatly different than that from very small-q^2 results. The significance of these results in Eqs. (9) and (10) may extend to astrophysics as well.

For a final comment, inelastic electrodisintegration data for $e + {}^3\mathrm{He} \to e' + X$ at large q^2 and $x = q^2/(2M_A\nu) \to 1$ will be useful, when available, to compare with $F_{^3\mathrm{He}}$. Continuity of the elastic and inelastic structure functions is predicted by parton-model analyses.[5,12]

In summary, the ratio of the measured ^{3}He form factor to the shape predicted by the quark-interchange model, $F_{^3\mathrm{He}}/F_{\mathrm{QIM}}$, changes slope for $q^2 > 2$ GeV^2, which I have interpreted as the onset of dimensional scaling. The ratio $F_{^4\mathrm{He}}/F_{\mathrm{QIM}}$ drops rapidly with $q^2 = 1.8$ GeV.[2] This investigation has led to the new results, as summarized by Eqs. (3), (4), and (10), which should be important guides in the synthesis of nuclear physics and quark-constituent ideas.

It is a pleasure to thank Professor S. J. Brodsky and Professor R. Blankenbecler for helpful discussions. This investigation was supported in part by the National Science Foundation, Grant No. PHY75-15986.

[1]S. J. Brodsky and B. T. Chertok, Phys. Rev. Lett. 37, 269 (1976).

[2]R. G. Arnold *et al.*, Phys. Rev. Lett. 40, 1429 (1978).

[3]S. J. Brodsky, R. Blankenbecler, and I. A. Schmidt, in *Proceedings of the Eigth International Symposium on Multiparticle Dynamics, Kaysersberg, France, 1977*, edited by R. Arnold, J. B. Gerber, and P. Schübelin (Centre de Recherches Nucléaires, Strasbourg, France, 1977); S. J. Brodsky, SLAC Report No. SLAC-Pub-2009 (unpublished); R. Blankenbecler and I. A. Schmidt, SLAC Report No. SLAC-Pub-2010 (unpublished); I. A. Schmidt, SLAC Report No. 203 (unpublished); R. Blankenbecler, S. J. Brodsky, and J. F. Gunion, Phys. Rev. D 18, 900 (1978).

[4]S. J. Brodsky and B. T. Chertok, Phys. Rev. D 14, 3003 (1976).

[5]An alternative extended model to that of Ref. 4 which uses dimensional counting and several other features has been developed by I. A. Schmidt and R. Blankenbecler, Phys. Rev. D 15, 3321 (1977), and especially Schmidt, Ref. 3.

[6]See Fig. 5 of Ref. 4.

[7]The last datum point at $q^2=3$ GeV^2 is 2 standard deviations above the exponential fit. Comparisons with inelastic data taken simultaniously indicate that this datum, representing a single event, could be a factor of 2 to 3 too large which would place the central value at or below the bottom of the error bar in Figs. 2 and 3. Private communication from S. Rock.

[8]F_{IA} in Fig. 3 is from Ref. 2 where it is credited as Ref. 14. Similar results are obtained using the variational calculation result from E. Hadjimichael, Nucl. Phys. A294, 513 (1978).

[9]The calculation of Ref. 4, Section II, is repeated for ^{3}He.

[10]It would be interesting to search for nine-quark-constituent effects in proton-deuteron elastic scattering, i.e., $s^{16}d\sigma/dt \rightarrow$ const near $\Theta=90°$. Incident protons with momenta ranging from 3 to 6 GeV/c should be suitable.

[11]V. A. Matveev and P. Sorba, Lett. Nuovo Cimento 20, 435 (1977), and FNAL Report No. FERMILAB Pub 77/56 (unpublished); A. P. Kobushkin, Ukrainian SSR Institute of Theoretical Physics Report No. 77-113E (to be published).

[12]W. P. Schütz *et al.*, Phys. Rev. Lett. 38, 259 (1977).

Role of the Exit-Channel Distorting Potential in Heavy-Ion–Induced Inelastic Scattering

R. J. Ascuitto, J. F. Petersen, and E. A. Seglie
Wright Nuclear Structure Laboratory, Yale University, New Haven, Connecticut 06520
(Received 28 July 1978)

The application of the distorted-wave Born approximation (DWBA) to inelastic scattering is examined. Particular attention is given to the $^{16}O+^{40}Ca$ system. The one-channel optical-potential wave function is found to be an adequate representation of the entrance-channel relative motion. The choice of exit-channel distorting potential DWBA is found to be crucial and a procedure to choose it correctly is discussed.

A recent Letter[1] emphasized the superiority of coupled-channels (CC) calculations to conventional distorted-wave Born-approximation (DWBA) calculations for the inelastic scattering to the lowest 2^+, 3^-, and 5^- states of ^{40}Ca by an ^{16}O projectile. The analysis of Ref. 1 showed that a conventional DWBA fails to describe the 5^- data, whereas a CC analysis succeeds, even though the coupling of the 5^- to either the 3^- or the ground state is weak. The success of the CC calculations was attributed to a more accurate treatment of the elastic-scattering wave function by the explicit coupling of the important inelastic channel (the 3^- of ^{40}Ca) to the ground state.

Such a feature, if general, would have profound consequences for heavy-ion–induced–transfer calculations since, even for a one-step transfer process involving nuclei with moderate inelastic collectivity, a CC calculation of inelastic scattering would be required in order to obtain an accurate description of the relative motion.

Fortunately, it is possible to view the results of Ref. 1 from a significantly different perspective, one in which the failure is *not* of the DWBA but only of what is called (in Ref. 1) the *conventional* DWBA (i.e., one in which the elastic-scattering optical potential is used as the exit-channel distorting potential). This conventional prescription, however, is clearly incorrect for many applications. We shall conclude from a direct comparison with the CC wave function that there is no serious problem associated with the adequacy of a one-channel optical-potential description of the elastic-scattering wave function. Rather, the error in the conventional DWBA is in the choice of the exit-channel distorting potential. In particular, this Letter will focus on the exit-channel distorting potential within the DWBA, and demonstrate that the distorted waves of the entrance and exit channels often must be calcu-

